Developmental Biology 387 (2014) 121–129

Contents lists available at ScienceDirect

Developmental Biology

journal homepage: www.elsevier.com/locate/developmentalbiology

Evolution of Developmental Control Mechanisms

The gap gene *Krüppel* of *Rhodnius prolixus* is required for segmentation and for repression of the homeotic gene *sex comb-reduced*

Andrés Lavore [a,b], Natalia Esponda-Behrens [a], Lucía Pagola [a], Rolando Rivera-Pomar [a,b,*]

[a] Laboratorio de Genética y Genómica Funcional, Centro Regional de Estudios Genómicos, Universidad Nacional de La Plata, Avenue Calchaqui Km 23.5, Florencio Varela, Buenos Aires, Argentina
[b] Centro de Bioinvestigaciones, Universidad Nacional del Noroeste de Buenos Aires, Pergamino, Argentina

ARTICLE INFO

Article history:
Received 11 December 2012
Received in revised form
18 December 2013
Accepted 20 December 2013
Available online 7 January 2014

Keywords:
Rhodnius
Krüppel
Gap gene
Segmentation
Hox regulation

ABSTRACT

The establishment of the anterior–posterior segmentation in insects requires the concerted action of a hierarchical gene network. Here, we study the orthologue of *Krüppel* gap gene in the hemipteran *Rhodnius prolixus* (*Rp-Kr*). We characterized its structure, expression pattern and function. The genomic sequence upstream of the *Rp-Kr* transcriptional unit shows a putative regulatory region conserved in the orthologue genes from *Drosophila melanogaster* and *Tribolium castaneum*. *Rp-Kr* expression is zygotic and it is expressed in the anterior half of the embryo (the posterior half of the egg) during the blastoderm stage and germ band formation; later, during germ band extension, it is expressed in a central domain, from T2 to A3. The *Rp-Kr* loss of function phenotypes shows disrupted thoracic and abdominal segmentation. Embryos with weak segmentation phenotypes show homeotic transformations, in which an ectopic tibial comb, typical of T1 leg, appears in T2, which correlates with the ectopic expression of *Rp-sex-comb reduced* in this leg.

Introduction

The embryogenesis of insects shows a diversity of mechanisms that always end up in the insect tagmata – head, thorax and abdomen. During the formation of the body insects develop in two main ways: short germ band and long germ band embryogenesis. In short germ band insects only the anterior segments are simultaneously specified during the blastoderm stage, while the posterior segments are successively added later on (reviewed in Liu and Kaufman (2005)). This mode of development is the most basal and widespread. However, most of our knowledge on developmental genetics comes from *Drosophila melanogaster*, a derived insect with long germ band embryogenesis. In *D. melanogaster* the anterior–posterior axis is determined by a hierarchical genetic network (reviewed in Rivera-Pomar and Jackle (1996)). The maternal genes are at the top of this network and define the expression of the gap genes, the first zygotic genes to be expressed to generate short overlapping gradients. In short germ band insects, these processes occur during early germ band, when the anterior segments are formed (reviewed in Liu and Kaufman (2005) and Peel et al. (2005)).

In *D. melanogaster* the mutants of the gap gene *Krüppel* (*Dm-Kr*) show loss and fusion of thoracic and abdominal segments (Wieschaus et al., 1984; Jackle et al., 1985). Dm-*Kr* encodes a transcription factor of the zinc-finger class (Rosenberg, et al., 1986), which is expressed in the central part of the blastoderm, region that corresponds to the thoracic and first abdominal segments (Jackle et al., 1985; Gaul et al., 1987). Beside *D. melanogaster*, *Kr* has been also studied in a few insects: *Gryllus bimaculatus*, *Oncopeltus fasciatus*, *Tribolium castaneum, Lucilia sericata* and *Apis mellifera* (Liu and Kaufman, 2004; Cerny et al., 2005; Mito et al., 2006; Wilson et al., 2010; Blechert et al., 2011). In these insects, *Kr* is expressed in the corresponding thoracic and first abdominal segments. In *O. fasciatus*, the lack of *Of-Kr* results in the loss of T2, T3 and some abdominal segments (Liu and Kaufman, 2004). In *G. bimaculatus* the absence of *Gb-Kr* results in a phenotypic series in which the most extreme interfered phenotype shows only one thoracic segment and the abdomen is reduced to a few segments (Mito et al., 2006). The *Of-Kr* and *Gb-Kr* interfered embryos phenotypes are similar to the *D. melanogaster* gap mutants, while in *T. castaneum*, the embryos devoid of *Tc-Kr* show segment deletion in the abdominal region and homeotic changes, where the thoracic and abdominal segments acquire gnathal identity. Thus, the *Kr* function varies in different insects.

Here, we present a detailed characterization of the *Krüppel* gap gene in the hemimetabolous insect *Rhodnius prolixus*, a short germ band insect, vector of the Chagas disease. We describe the structure and function of the *Rp-Kr* gene. We show that *Rp-Kr*

* Corresponding author at: Centro de Bioinvestigaciones, Universidad Nacional del Noroeste de Buenos Aires, Pergamino, Argentina
E-mail addresses: rrivera@unnoba.edu.ar, rrivera@gwdg.de (R. Rivera-Pomar).

0012-1606/$ - see front matter © 2013 Elsevier Inc. All rights reserved.
http://dx.doi.org/10.1016/j.ydbio.2013.12.030

expression occurs in the central region of the embryo, which correlates with the result of parental RNAi experiments that affects segmentation of the middle embryonic region. We also show that *Rp-Kr* acts upstream the homeotic gene *sex-combs reduced*.

Material and methods

Insect rearing

The colony of *R. prolixus* was maintained in our laboratory in a 12 h light/dark schedule at 30 °C and 70% humidity. In these conditions the embryogenesis takes 14 ± 1 days. The insects were regularly fed *ad libitum* on chickens once or twice before molting. When necessary, V larval instars were sexed before molting until adulthood and then mated.

Identification and cloning of the Rp-Kr gene

The strategy for gene discovery in the *R. prolixus* genome has already been described (Ons et al., 2010; Lavore et al., 2012). Traces of *R. prolixus* whole genome sequence (WGS), EST and WGS assembly databases were used for homology search by local TBLASTN. *R. prolixus* genomic data was produced by Washington University School of Medicine in St. Louis as part of the *R. prolixus* Genome Project and are currently deposited in Vector Base (www.vectorbase.org). A set of specific primers was designed spanning the five zinc-finger domains either containing or not the T7 promoter sequence (underlined below) at the 5′ end for further use in *in vitro* transcription.

KrFwT7: CGACTCACTATAGGGTGTGCAGGGTGTGTAACCATTC,
KrRvT7: CGACTCACTATAGGGAGAAGGGTTTTTCACCACGATG,
KrFw: AAAATCACGAACGAACCCACAC,
KrRv: CGTTCTCCGGTGTGTACCCTTAG.

The expression of *Rp-Kr* was confirmed by PCR on standard and normalized embryonic cDNA libraries (data not shown). The amplicons were cloned into the vector pGEM-T Easy (Promega) and several independent clones were sequenced.

Sequence analysis

Prediction of the gene structure and open reading frame on the genomic sequence was done with Lasergene (DNASTAR) and by manual curation. *Rp-Kr* sequence was aligned with the *Kr* orthologues from different insects using Clustal W. This alignment was used for phylogenetic analysis employing the centipede *Strigmia maritima* as outgroup. Phylogenetic analysis was performed using the Bayesian algorithm, Mr. Bayes Online http://www.phylogeny.fr (Dereeper et al., 2008; Huelsenbeck et al., 2001). The parameters used for the analysis were: number of substitution types: 6(GTR), substitution model: Blosum62, number of generations: 100.000 and a sample tree every 10 generations.

A larger genomic fragment was assembled using traces containing the partial *Rp-Kr* ORF. For putative regulatory regions we analyzed 5 Kbp upstream of the *Rp-Kr* ORF. The software PATSER (http://rsat.ulb.ac.be/rsat/patser_form.cgi) was employed for searching each transcription factor binding sites that match in the genomic sequence using the Position Weight Matrices (PWMs) described by Berman et al. (2002) and Lavore et al. (2012). The parameters used were: lower threshold estimation – weight store: 5; alphabet: a:t 0.297 c:g 0.203. As validation methods. We also analyzed the presence of clustered binding sites using the software STUBB (http://stubb.rockefeller.edu/).

Embryonic techniques and RNA in situ hybridization

Embryos were collected at different times after egg laying (AEL) (24, 36 and 48 h AEL). The staging was as the one described by Esponda-Behrens et al. (submitted for publication). The dissection and fixation of embryos was performed as described in Lavore et al. (2012). Embryo *in situ* hybridization technique is described elsewhere (Esponda-Behrens et al., submitted for publication). The embryos were counterstained with DAPI for staging. Images were acquired either with a fluorescence microscope or a binocular stereoscope (Leica DM 1000; Leica FLZIII) and a CCD camera, Cool SNAP-Procf color (Media Cybernetics).

RNAi

dsRNA was produced by simultaneous T7 RNA polymerase transcription on PCR products containing T7 promoter sequences at both ends of the *Rp-Kr* ORF. For every independent experiment we used dsRNA corresponding to the beta-lactamase gene of *E. coli* as a negative control. dsRNA was quantified and injected in virgin females (2.0 μg per insect in no more than 5 μl) as described in Lavore et al. (2012). After 2–3 days post injection, the females were fed to induce oogenesis. After mating, the eggs were collected from individual females. Embryos were immediately fixed or let to develop to account for lethality and/or cuticle preparation. Cuticles were prepared as described in Lavore et al. (2012). Cuticle morphology was performed taking advantage of autofluorescence in the 520–660 nm range. Images were acquired using a Zeiss 510-META confocal microscope at 488 nm excitation/535 nm emission. A maximum projection images were generated from 15 image stacks.

Results

Isolation and characterization of Rp-Kr orthologue

To identify the *Krüppel* orthologue in *R. prolixus* we performed an homology search on *R. prolixus* whole genome trace archives. We identified several incomplete scaffolds that were assembled into a 53.6 Kpb genomic region. The *Rp-Kr* gene region spans 14.8 Kpb (Gene Bank JN092576), showing a 339 amino acid ORF with high similarity to the known *Kr* orthologues in other insects. To validate the expression of the bona fide *Rp-Kr* gene, we designed specific primers within the ORF spanning Zinc Fingers (ZnF) 1–4 and we performed PCR on cDNA derived from *R. prolixus* embryos. A PCR product of 336 bp was obtained (not shown) and sequenced to confirm the identity of a *Rp-Kr* transcript (Gene Bank GU724144.1). The *Rp-Kr* gene is composed by three exons of 421 pb, 281 pb, and 281 pb in length (Fig. 1). The protein sequence was compared to the available *Kr* orthologues and it showed the highest sequence similarity within the ZnF 1–5 region. In addition, a second conserved domain could be identified among insects, with no biological function assigned yet (Fig. 2A). The evolutionary analysis revealed that *R. prolixus* and *O. fasciatus* form a monophyletic group and that the species distribution fit well with the evolution of the Class Insecta – except *T. castaneum* that is not grouping within the holometabola clade (Fig. 2B).

The analysis on 5 Kpb genomic region upstream of the *Rp-Kr* transcriptional unit has revealed regulatory features. The bioinformatic analysis using the PATSER software showed several binding sites for putative transcriptional regulators: Hb, 40; K-50 homeodomain class (Bcd/Otd/Six), 10; Cad, 26; Kr, 7; Kni, 12 and Gt, 16. As the presence of binding sites could occur at random, we have also analyzed the clustering using the software STUFF. We could predict two clusters of binding sites: one between −1

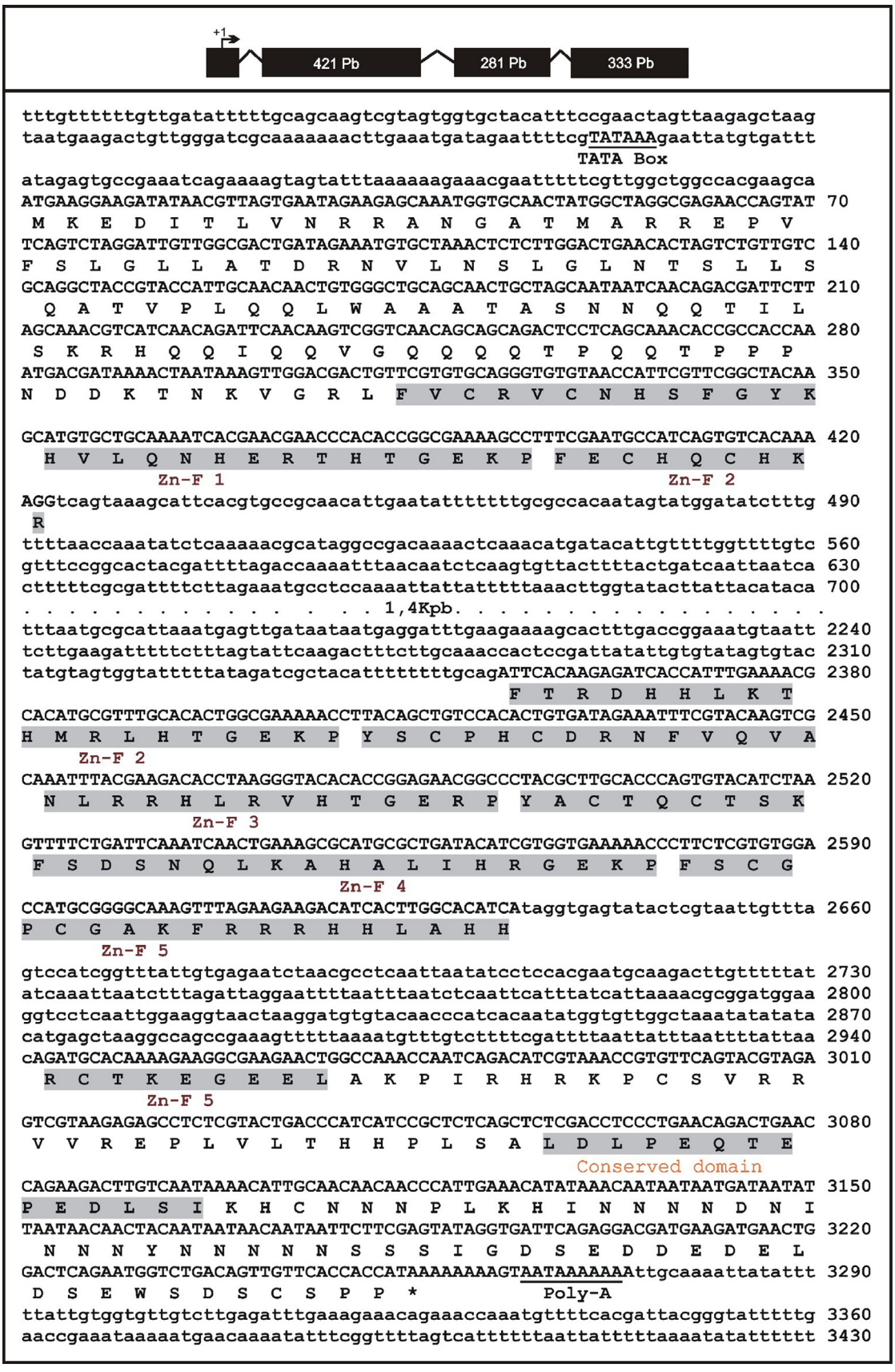

Fig. 1. The *Rp-Kr* gene. Upper panel, graphic representation of *Rp-Kr* gene. Black boxes represent the exons; the numbers the exon length. Lower panel, nucleotide and protein sequence of *Rp-Kr*. The conserved protein domains Zn-F 1–5 and the additional conserved domain are shadowed in gray. The putative TATA-Box, transcription initiation site and the polyadenilation signal are underlined. The exonic regions are in capital letters and the introns in lower case.

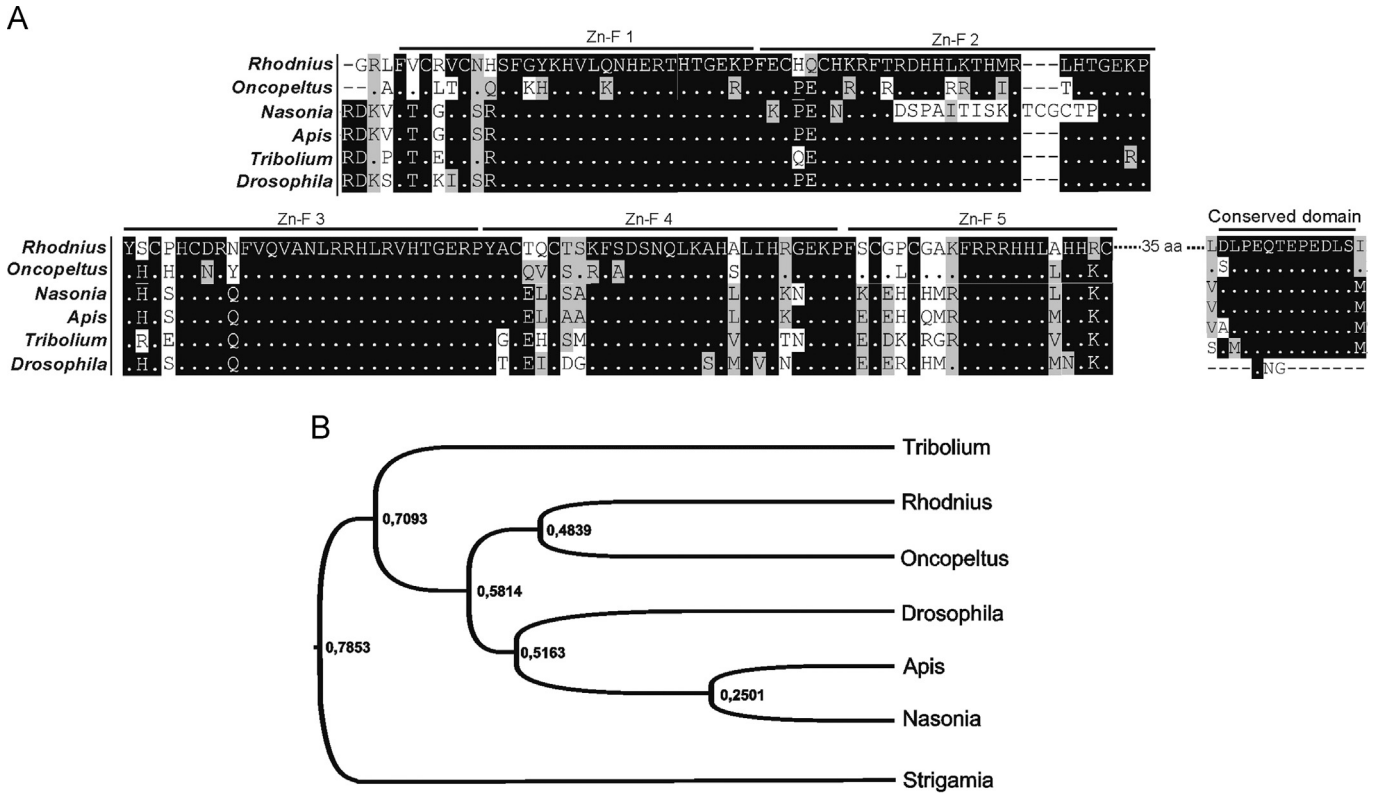

Fig. 2. *Rp-Kr* gene analysis. A. Alignment of *Rp-Kr* protein with other insect orthologues. Black boxes indicate complete identity. B. Phylogenetic analysis of *Rp-Kr*. The tree was generated by Bayesian phylogenetic inference; the node values indicate the clade credibility values.

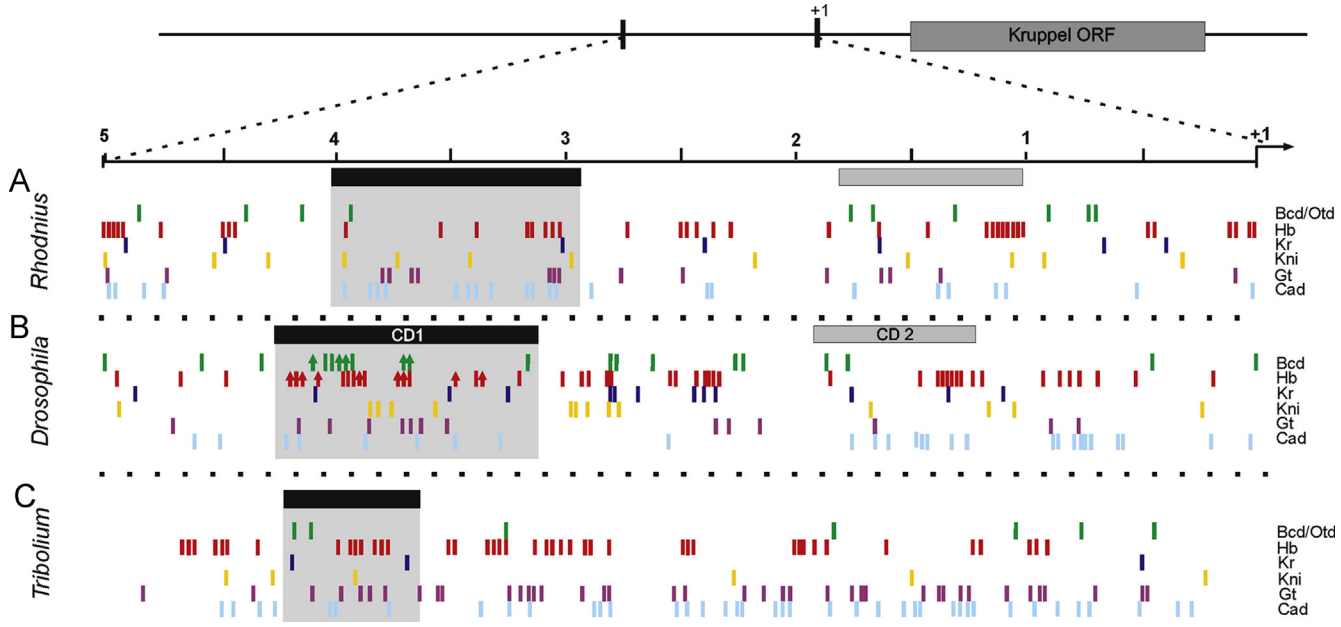

Fig. 3. Comparative analysis of the putative *Kr* regulatory region in *R. prolixus*, *T. castaneum* and *D. melanogaster*. The analysis was applied both to the *Kr* upstream sequences of *R. prolixus* (A), *D. melanogaster* (B) and *T. castaneum* (C). The different potential transcriptional regulators are indicated on the right side. The color bars represent different binding sites for the transcription factors as predicted by the software PATSER. The black (highest probability) and gray boxes mark the predicted clusters of binding sites according to the software STUBB. The scale represents 1 Kbp. Note that the predicted clusters for *D. melanogaster* coincide with the empirically defined enhancers CD1 and CD2 (Hoch et al., 1990). The binding sites marked with arrows in the *D. melanogaster* prediction represent coincidence with the experimental data.

and −1.7 Kpb upstream of the putative transcription start and a second one between −3 and −4 Kpb, the latter including Bcd/Otd, 1; Hb, 8; Kr, 1; Kni, 4; Gt, 7 and Cad, 12 (Fig. 3A). To evaluate the reliability of our analysis on *Rp-Kr*, we have also analyzed the clustering pattern in the *D. melanogaster* and *T. castaneum Kr* genomic upstream regions. *Dm-Kr* was used as a control due to the experimental demonstration of their regulatory regions (Hoch et al., 1990). We could determine a cluster between −3.7 and −4.3 Kpb upstream of the transcriptional start in *Tc-Kr* (Fig. 3C) and two regulatory clusters in *Dm-Kr* (Fig. 3B), which are coincident to the regulatory regions identified by Hoch et al. (1990). The first of these clusters is located between −3 and −4.3 Kpb upstream from the

transcription start site – similar position to CD1 – and the second one between −1.3 and −2 Kpb – similar position to CD2. We have noted that at least one cluster of regulators is conserved in quality of binding sites and in the relative position in the three species, this corresponds to *Dm-Kr* CD1. The similarities shown between the *Dm-Kr* prediction and the experimental evidence support the predictions on *R. prolixus* and *T. castaneum*, thus we consider that we have defined bona fide conserved regulatory regions for *Rp-Kr* and *Tc-Kr*.

Rp-Kr expression in the embryo

We have performed *in situ* hybridization in *R. prolixus* embryos using an antisense RNA probe targeting the *Rp-Kr* ORF and studied different developmental stages: from early eggs (0–12 h AEL) to fully extended germ band stages (48–60 h AEL). *Rp-Kr* expression is zygotic; the transcript could not be revealed before 30 h AEL (Fig. 4). During the blastoderm stage (30–36 h AEL), the expression domain is evident in the anterior part of the embryo accompanying the migration of the cells that will form the germ band (Fig. 4A and B; note that the anterior part of the embryo corresponds to the posterior part of the egg before katatrepsis). In the ventral side, *Rp-Kr* transcript is expressed in the anterior half of the embryo (posterior of the egg), forming a gradient (Fig. 4A and A′). At this developmental stage, the expression domain splits in the dorsal side near to the invagination center (Fig. 4B and B′). During early germ band stage (40 h AEL), *Rp-Kr* shows two expression domains: an anterior and a central one. The anterior domain, which is transiently expressed, corresponds to the cephalic lobes. The central expression domain is located in the presumptive region corresponding to the thoracic segments (Fig. 4C and D). After germ band extension (48–60 h AEL) a strong expression of *Rp-Kr* mRNA could be observed in the middle region of the embryo corresponding to the segments T2 to A2 (Fig. 4E–G). The segment identity is based-on the morphological definition of the embryonic segments and it has been used instead of molecular

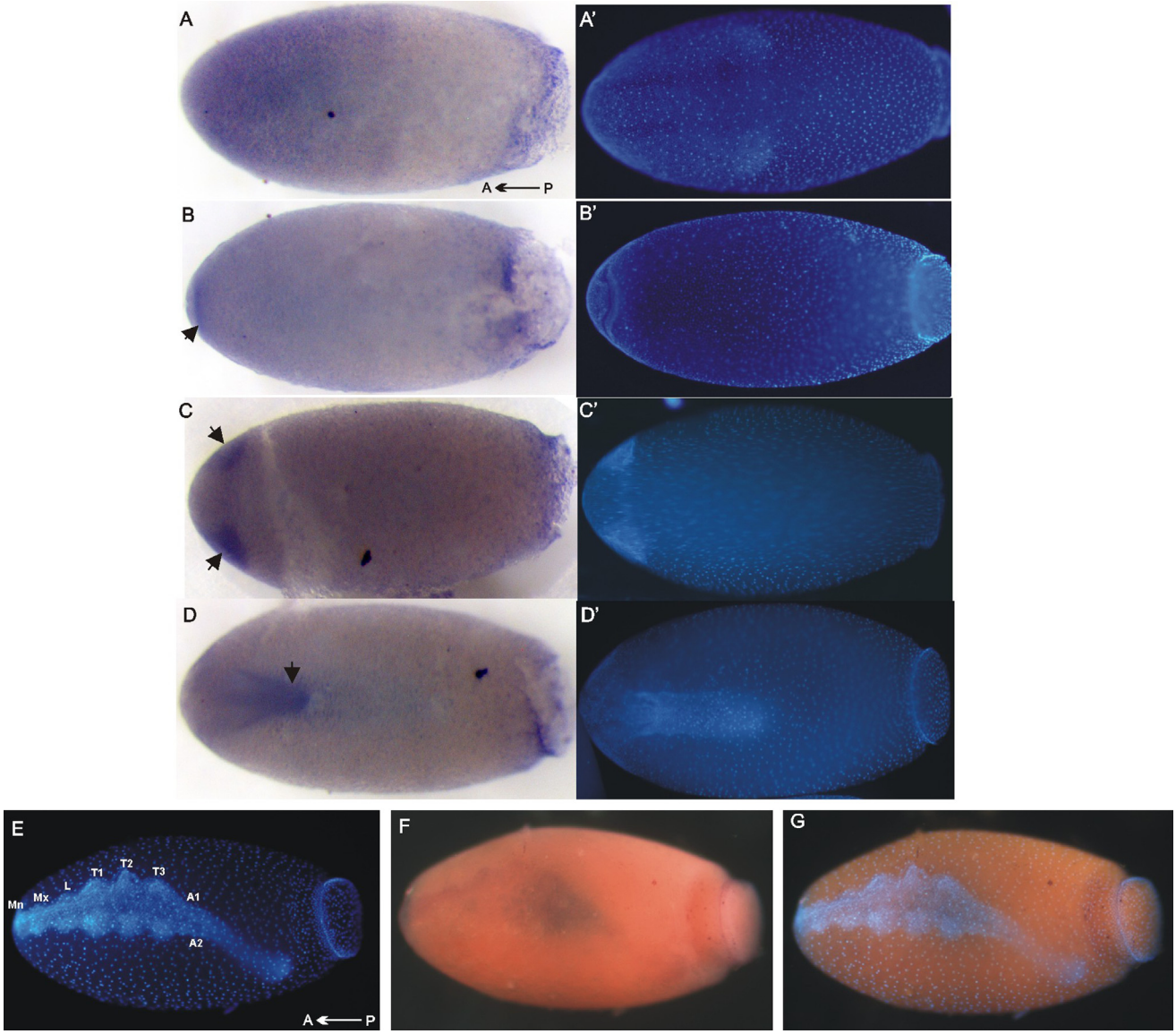

Fig. 4. Expression of *Rp-Kr* by whole mount *in situ* hybridization. A–B′. Early embryo in the invagination stage (30–36 h AEL). A. Ventral view showing the transcript distribution in the anterior pole of the embryo (the A–P arrow marks embryo′s anterior pole). B. Dorsal view of the same stage showed in A. The arrow marks the invagination border; note the higher expression of the *Rp-Kr* transcript. A′ and B′. The same embryo in A and B staining with DAPI. C–D′. Embryo during the early germ band stage (40 h AEL). C and C′. Ventral view, *Rp-Kr* transcript is located in the cephalic lobes. D and D′. Dorsal view, the transcript is located in the middle region of the embryo. E–G. Ventral view of an extended germ band embryo at 48–60 h AEL. E. DAPI-stained embryo indicating the head and thoracic segments (Mn, mandible; Mx, maxillae; Lb, labium; T1–T3, thoracic segments 1–3). F. Distribution of *Rp-Kr* transcript in the same embryo shown in F. G. Merged image by double exposure by epiillumination with visible light and UV epifluorescence showing the expression of the *Rp-Kr* transcript from T2 to the first abdominal segments.

markers (such as segment polarity gene markers), because double *in situ* hybridization has been technically impossible to up to date. Later on – in the same way that in other insects – the expression of *Rp-Kr* becomes ubiquitous (not shown).

Table 1
Parental RNAi of *Rp-Kr*.

	Strong (%)	Weak (%)	WT (%)	Total
Number of embryos	201 (96%)	3 (1.6%)	5 (2.4%)	209 (100%)

Rp-Kr phenotype

To study the lack-of-function phenotype of *Rp-Kr*, we have generated knock-down embryos by parental RNAi. Injected females laid a total of 279 eggs from three independent experiments. All embryos derived from interfered females were lethal, however, they completed the development. The embryos were studied at different developmental stages and a major fraction ($n=209$) was analyzed for *Rp-Kr* cuticle phenotype (Table 1). 98% of the interfered embryos showed a segmentation phenotype compared to the wild-type and the β-lactamase-injected control insects. The RNAi phenotypes were separated in two groups: weak (2%) and strong (98%) phenotypes. All the embryos showed an

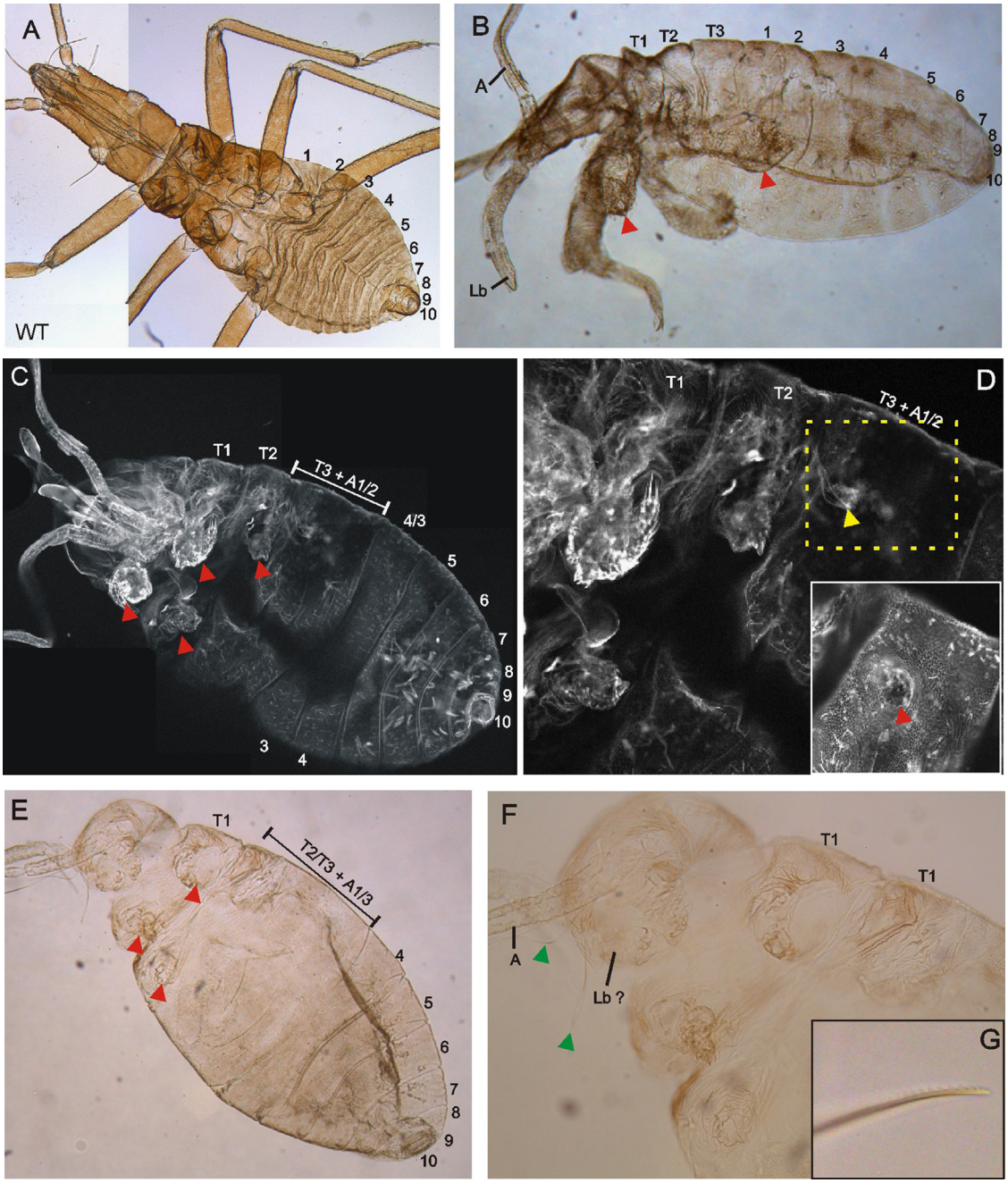

Fig. 5. *Rp-Kr* RNAi phenotype. A. *R. prolixus* wild type first instar larva. Cuticle preparation in dorsal view indicating the ten abdominal segments. B. Weak *Rp-Kr* phenotype. First instar larva in lateral view; note that all segments are present, but the thoracic appendages are reduced (T1, T2) or absent (T3). C–G. Strong *Rp-Kr* phenotype. C. Confocal image of a larva showing loss and fusion of T3 to A1–2; A3 and 4 are partially fused. D. Magnified view of C. The inset shows T3 leg primordium. The apodemes are indicated with the yellow arrowhead. E. Extreme gap phenotype from T2 to A3. The labium, as in image C, is affected. F. Magnification of the larval head from E showing the labial modification. The arrowhead marks the stylets. G. Detail of a mandibulary appendage. Note the normal serrated morphology. A, antenna; Lb, labium.

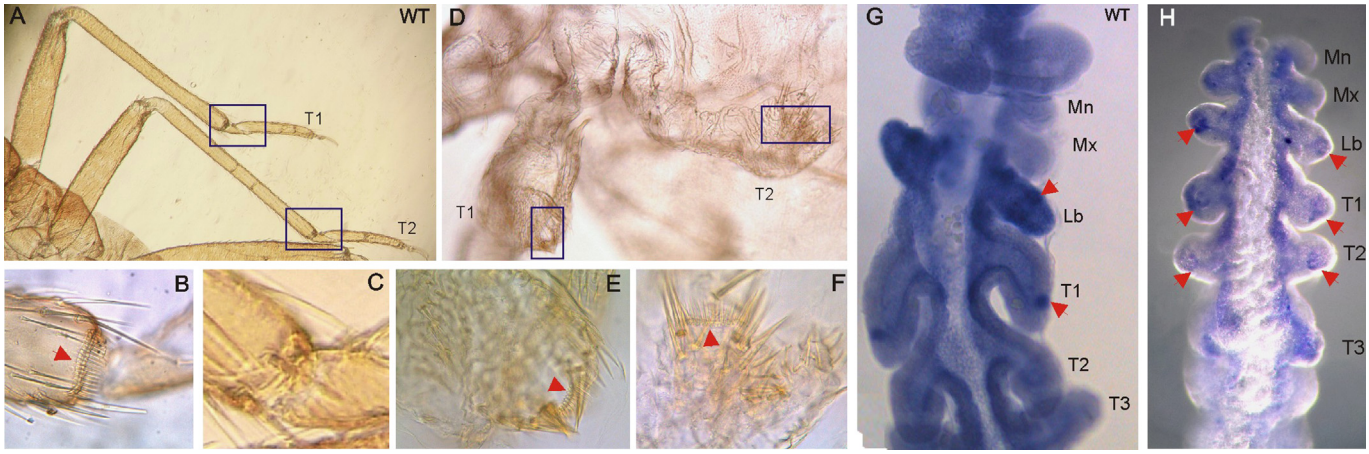

Fig. 6. Homeotic changes in *Rp-Kr* interfered embryos. A. Wild type first instar larva T1 and T2 legs. The rectangles mark the distal tibial region, magnified in B and C. B. Detail of the tibial comb present in the T1 leg. C. Distal tibial region of a T2 leg, in which the tibial comb is not present. D. T1 and T2 legs in a *Rp-Kr* interfered larva. The rectangle indicates the position of the tibial combs. E. Magnification of the T1 tibial comb shown in B. F. Magnification of the residual leg in T2. Note the position of the tibial comb (arrow head). G. *Rp-Scr* pattern expression in a wild type germ band embryo. Note the expression in the Labial (Lb) and T1 segment. H. *Rp-Scr* expression in a *Rp-Kr* interfered embryo. The transcript is expressed in the Lb and T1 segment and in T2 in a pattern such as in T1. Note the reduction of appendage and disarray of T3 and first abdominal segments. Lb, labium; Mn, mandible; Mx, Maxilla.

unequivocal and consistent phenotype in the thoracic and abdominal segments (Fig. 5).

The weak phenotype embryos presented normal development of the cephalic and abdominal segments but the thorax was affected (Fig. 5B). Cuticle analysis of cleared larvae and/or fluorescent confocal optical sections showed that the thoracic segments are still formed but their appendages are reduced or absent. In these embryos, the T1 and T2 segments develop reduced legs, while T3 lacks the appendages. Fig. 5B shows that the *Rp-Kr* phenotype is stronger in the posterior thoracic segments, which corresponds to the *Rp-Kr* expression domain as revealed by *in situ* hybridization.

The strong phenotype embryos ($n=201$) show a dramatic alteration of the head morphology and the thorax segmentation compared to the wild type and control (Fig. 5C–G). The thoracic appendages are strongly reduced and T3 segment is fused to A1 and, sometimes, also the A2 segments (Fig. 5C and D). Fig. 5C shows an embryo in which the A3 and A4 are partially fused, while A1 and A2 are fused to the thoracic segment forming a gap. By confocal imaging we detected within this T3–A2 gap a cuticular structure similar to an appendage bud (see inset in Fig. 5D) including an apodem-like structure (yellow arrow head in Fig. 5D; apodems are the attachment sites of the appendage muscle). We cannot unequivocally establish the identity of the appendage, however, we consider that it corresponds to leg 3, suggesting that the affected thoracic/abdominal region still has the ability of generating appendages (Fig. 5C and E). In the most extreme phenotypes (70% of the larvae with strong phenotype), the central body part is coalescent from T2 to A3 (Fig. 5D). In consequence, the number of abdominal segments is reduced from 10 (wild type) to 7 (Fig. 5D and E). In addition, we observed that all the embryos that show the strong phenotype display a proboscis deformation that only affects the labium, while the stylets are normally developed (Fig. 5G). The alterations in the cephalic region could be attributed to the miss regulation of *Rp-Kr* target genes during the formation of the head segments in early stages and before the establishment of the *Rp-Kr* central domain.

Rp-Kr homeotic phenotype

Besides the segmentation phenotype, *Rp-Kr* RNAi embryos show homeotic transformations. The wild type insects exhibit a group of stiff setae in the tibia of the T1 leg, forming a tibial comb (Fig. 6A and B), while T2 and T3 legs lack of any tibial comb (Fig. 6C) and this can be considered as a homeotic difference between the first and second thoracic segment. In the interfered insects with weak phenotype, the T1 tibial comb is still present (Fig. 6D and E) and an ectopic tibial comb can be observed in the remaining of the second thoracic leg (Fig. 6D and F). Therefore, the interfered insects develop tibial combs in T1 as well as T2 legs, indicating a homeotic transformation in these segments.

Sex combs-reduced is a conserved homeotic gene related to the presence of tibial combs (Patatucci et al., 1991). In *R. prolixus*, *Rp-Scr* is expressed in T1 leg primordimum (Esponda-Behrens et al., submitted for publication), thus, we have analyzed the expression of *Rp-Scr* in *Rp-Kr* interfered embryos. Compared to the wild type expression, as assessed by *in situ* hybridization (Fig. 6G), *Rp-Scr* is ectopically expressed in T2 of fully extended germ band *Rp-Kr* interfered embryos (Fig. 6H). The ectopic expression of *Rp-Scr* in T2 leg shows the patched pattern observed in the distal part of T1 leg of the wild type embryo, which corresponds to the tibial article. Therefore, the ectopic *Rp-Scr* expression correlates with the ectopic tibial comb in T2 leg and suggests that *Rp-Kr* represses the pro-thoracic identity of the T2 segment.

Discussion

In the present work, we analyzed the structure, expression and function of the orthologue gene *Krüppel* in *Rhodnius prolixus*. *Krüppel* is a highly conserved gap gene among insects. In *R. prolixus*, the *Kr* orthologue encodes a transcription factor that contains the five Zn-finger domains described for *D. melanogaster* (Rosenberg, 1986) that are strictly conserved among insects (Liu and Kaufman, 2004; Cerny et al., 2005; Mito et al., 2006; Wilson et al., 2010).We have also defined a novel protein domain conserved in other insects, however, a biological function for this protein domain is still unknown.

The similarity also extends to the genomic region upstream of the transcription start. In *D. melanogaster*, the transcriptional regulation of the gap genes was studied in detail, while in other insects the information is still scarce. Particularly, the regulation of *Kr* has been studied in detail in *D. melanogaster* (Hoch et al., 1990, 1991). Two enhancers were characterized in *Dm-Kr*, namely CD1 and CD2. CD1 acts during the early stages of *Kr* expression while CD2 regulates *Kr* expression later in development. The binding sites for different transcription factors and their interaction were established in CD1 using *in vitro* and *in vivo* approaches (Hoch et al., 1991). By comparative genomic analysis, we have identified a

putative regulatory region for *Rp-Kr*, *Tc-Kr* and *Dm-Kr*, which we used as a reference for our analysis. We were able to predict two clusters of binding sites in *Dm-Kr* that coincide with the empirically defined CD1 and CD2 regions. This supports our robust prediction, which resulted in a similar clustering pattern for the transcription binding sites in the species studied. Our results suggest a conserved regulatory region in *Rp-Kr*, *Tc-Kr* and *Dm-Kr*. In this regard, we have recently shown the conservation of putative regulatory regions for the gap gene *giant* of *R. prolixus* (Lavore et al., 2012). Taken together, these analyses suggest that the conservation of regulatory regions, at least for gap genes, is not as uncommon as we could have expected for insects largely separated during evolution and with different developmental modes. These provide a theoretical background for comparative genome analysis of regulatory regions – identified in *R. prolixus* – that still need to be confirmed by functional analysis in our novel model organism as new techniques are available. As the studies of transcriptional regulation in insects are still scarce the data presented here represents a first step towards that goal, necessary to understand the evolution of the segmentation process.

Krüppel expression and function

D. melanogaster, L. sericata and *A. mellifera* are the only long germ band insects in which *Kr* has been studied so far. *Dm-Kr* expression is always zygotic and occurs from T2 to A1 in the blastoderm. Mutants of *Dm-Kr* result in a phenotypic series that affects thoracic and first abdominal segments, in which only the last three caudal segments persist remain (Wieschaus et al., 1984; Preiss et al., 1985). *Ls-Kr* shows a slightly different expression compared to *Dm-Kr*, but the gap phenotype is conserved (Blechert et al., 2011). *Am-Kr* expression also occurs in a central domain during the sincitial blastoderm stage, and later on it splits in an anterior, middle and posterior domain. The expression became generalized from the 6th developmental stage on Wilson et al. (2010). The lack of *Am-Kr* results in a segmentation phenotype spanning from T1 to A6. *Kr* has also been studied in short germ band insects such as *T. castaneum*, *G. bimmaculatus* and *O. fasciatus* (Liu and Kaufman, 2004; Cerny et al., 2005; Mito et al., 2006). *Tc-Kr* is expressed in the most posterior part of the egg during the blastoderm stage and in T1–T3 during the germ band stage (Cerny et al., 2005). The allele *jaws* – a mutant of *Tc-Kr* – lacks or fuses thoracic and abdominal segments and shows a cephalized homeotic phenotype (maxillae and labium develop in thoracic and abdominals segments respectively). In *G. bimaculatus* and *O. fasciatus* the expression is limited from T1 to T3 – *Gb-Kr* is also expressed in the labial segment. The lack of *Of-Kr* and *Gb-Kr* result in thoracic and abdominal segments deletions, while the cephalic region remains unaltered (Liu and Kaufman, 2004; Mito et al., 2006). In *R. prolixus*, *Kr* expression occurs early during the blastoderm and germ band formation (30–36 h AEL). *Rp-Kr* transcript is expressed in the anterior half of the embryo and it follows the migration of the cells that will form the germ band. A more intense signal is observed near the invagination border. A similar expression was observed in *T. castaneum* and *O. fasciatus*. During early germ band stage, *Rp-Kr* is expressed in two domains: one in the cephalic lobes and the other in the presumptive thoracic region. The anterior *Kr* expression domain has also been described in other insects but it does not seem to affect the head segmentation (Liu and Kaufman, 2004; Cerny et al., 2005; Mito et al., 2006). Although we could not determine a head gap phenotype, the interfered insects show a consistent defect of the labium. A single *Rp-Kr* domain is visible at the completion of the germ band extension from T2 to A2–3 and it correlates with the segment disarray from T2 to A3 observed in the interfered insects. This phenotype resembles the classic gap phenotype of *Dm-Kr* mutants (Wieschaus et al., 1984; Preiss et al., 1985). In the weak *Rp-Kr*

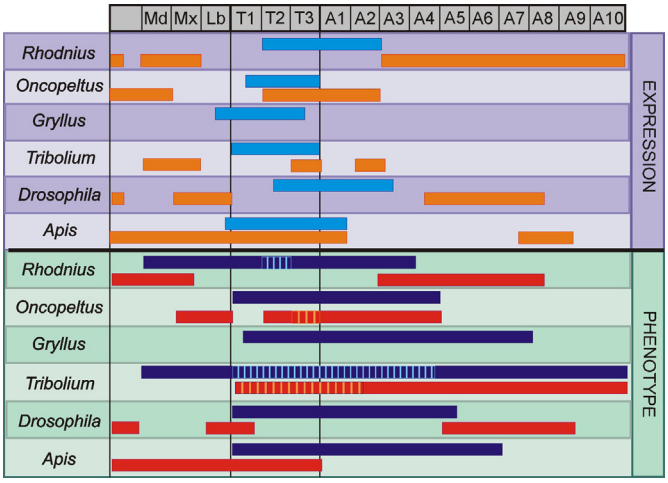

Fig. 7. *Kruppel* and *giant* expression domains and phenotype comparison between *R. prolixus*, *T. castaneum*, *D. melanogaster*, *G. bimaculatus*, *A. mellifera* and *O. fasciatus*: A. Expression domains of *Kr* (light blue bars) and *gt* (orange bars). B. Body regions affected due to the lack of *Kr* and *gt* expression (blue and red bars respectively). The solid bars mark the body regions in which the embryo shows lack or fusion of segments. The tiger bars mark corporal regions with homeotic changes in absence of these genes.

interfered embryos the thoracic but not the abdominal region is affected. Thus, the thoracic segments seem to be more sensitive than the abdominal ones to small changes in the *Rp-Kr* expression levels. Fig. 7 shows a comparative summary of gap gene expression patterns between *D. melanogaster*, *T. castaneum*, *G. bimaculatus*, *A. mellifera*, *O. fasciatus* and *R. prolixus*. It shows that *R. prolixus* shares many similarities with some insect species, showing that different mechanism of development ends always in the same morphological pattern. Whether this is solely restricted to gap genes is still to be determined.

The regulation of the Hox genes by the gap genes has been widely studied in *D. melanogaster*. In *T. castaneum*, the mutant *jaws* changes the identity of thoracic and abdominal segments for head segments – the thoracic and abdominal segments develop Mx and Lb appendages (Cerny et al., 2005). This is the result of the deregulation of the Hox gene in the cephalothorax – *Tc-Scr* and *Tc-Antp* – as a result of the change of the expression pattern of *Tc-giant* when *Tc-Kr* is absent. In *O. fasciatus*, homeotic changes were also observed when *Of-gt* is absent, but not in *Of-Kr* insects. In *Of-gt* interfered embryos the T3 leg develops an ectopic tibial comb as the result of the ectopic expression of *Of-Scr* in the third thoracic segment (Liu and Patel, 2010). *Rp-Kr* interfered embryos develop an ectopic tibial comb in the T2 leg as a result of the derepression of *Rp-Scr*. In the *R. prolixus* wild type embryos, *Rp-Scr* is expressed in the labium and in the T1 leg, where it is required for the formation of the T1 tibial comb (Esponda-Behrens et al., submitted for publication). Different to *O. fasciatus*, in which *Of-Scr* is indirectly derepressed by *Of-Kr* through *Of-gt*, we did not observe homeotic changes in RNAi *Rp-gt* insects (Lavore et al., 2012) and, therefore, we propose a direct repression effect of *Rp-Kr* on *Rp-Scr* in T2. This shows that relatively close species such as *O. fasciatus* and *R. prolixus* do not necessarily share similar regulatory mechanisms to pattern equivalent bodies. As the genome of *O. fasciatus* is not yet known, we could not compare regulatory elements among species as we have done for genes such as *Rp-gt* (Lavore et al., 2012), *Rp-Scr* (Esponda-Behrens et al., submitted for publication) or *Rp-Kr* in this work.

R. prolixus, a classical model for insect physiology, is emerging as a model for insect development due to the advances in the sequencing of its genome. In the Class Insecta, most of the genes that take part in the segmentation process are conserved but their function and regulation is not always retained – and that is the case of *Kr*. Further comparative and functional genomic analysis will provide more solid

basis to understand the patterning process in an evolutionary framework.

References

Berman, B.P., Nibu, Y., Pfeiffer, B.D., Tomancak, P., Celniker, S.E., Levine, M., Rubin, G. M., Eisen, M.B., 2002. Exploiting transcription factor binding site clustering to identify cis-regulatory modules involved in pattern formation in the *Drosophila* genome. Proc. Natl. Acad. Sci. USA 99, 757–762.

Blechert, O., Douglas, D., Baumgartner, S., 2011. Conserved function of the Kruppelgap gene in the blowfly Lucilia sericata, despite anterior shift of expression. Insect Mol. Biol. 20, 257–265.

Cerny, A.C., Bucher, G., Schroder, R., Klingler, M., 2005. Breakdown of abdominal patterning in the *Tribolium Krüppel* mutant jaws. Development 132, 5353–5363.

Dereeper, A., Guignon, V., Blanc, G., Audic, S., Buffet, S., Chevenet, F., Dufayard, J.F., Guindon, S., Lefort, V., Lescot, M., Claverie, J.M., Gascuel, O., 2008. Phylogeny.fr: robust phylogenetic analysis for the non-specialist. Nucleic Acids Res. 36, W465–W469.

Gaul, U., Seifert, E., Schuh, R., Jackle, H., 1987. Analysis of *Krüppel* protein distribution during early *Drosophila* development reveals posttranscriptional regulation. Cell 50, 639–647.

Hoch, M., Schroeder, C., Seifert, E., Jackle, H., 1990. Cis-acting control element for *Krüppel* expression in the *Drosophila* embryo. EMBO J. 9, 2587–2595.

Hoch, M., Seifert, E., Jackle, H., 1991. Gene expression mediated by cis-acting sequences of the *Krüppel* gene in response to the *Drosophila* morphogens *bicoid* and *hunchback*. EMBO J. 10, 2267–2278.

Huelsenbeck, J.P., Ronquist, F., Nielsen, R., Bollback, J.P., 2001. Bayesian inference of phylogeny and its impact on evolutionary biology. Science 294, 2310–2314.

Jackle, H., Rosenberg, U.B., Preiss, A., Seifert, E., Knipple, D.C., Kienlin, A., Lehmann, R., 1985. Molecular analysis of *Krüppel*, a segmentation gene of *Drosophila melanogaster*. Cold Spring Harb. Symp. Quant. Biol. l50, 465–473.

Lavore, A., Pagola, L., Esponda-Behrens, N., Rivera-Pomar, R., 2012. The gap gene *giant* of *Rhodnius prolixus* is maternally expressed and required for proper head and abdomen formation. Dev. Biol. 361, 147–155.

Liu, P.Z., Kaufman, T.C., 2004. *Krüppel* is a gap gene in the intermediate germband insect *Oncopeltus fasciatus* and is required for development of both blastoderm and germband-derived segments. Development 131, 4567–4579.

Liu, P.Z., Kaufman, T.C., 2005. Short and long germ segmentation: unanswered questions in the evolution of a developmental mode. Evol. Dev. 7, 629–646.

Liu, P.Z., Patel, N.H., 2010. *giant* is a bona fide gap gene in the intermediate germband insect, *Oncopeltus fasciatus*. Development 137, 835–844.

Mito, T., Okamoto, H., Shinahara, W., Shinmyo, Y., Miyawaki, K., Ohuchi, H., Noji, S., 2006. *Krüppel* acts as a gap gene regulating expression of *hunchback* and *even-skipped* in the intermediate germ cricket *Gryllus bimaculatus*. Dev. Biol. 294, 471–481.

Pattatucci, A.M., Otteson, D.C., Kaufman, T.C., 1991. A functional and structural analysis of the sex combs reduced locus of *Drosophila melanogaster*. Genetics 129, 423–441.

Preiss, A., Schmidt-ott, U., Kienlin, A., Seifert, E., Jackle, H., 1985. Molecular Gentics of *Kruppel*, a gene requiered for segmentation of the *Drosophila* embryo. Nature 313, 27–32.

Rivera-Pomar, R.V., Jackle, H., 1996. From gradients to stripes in *Drosophila* embryogenesis: filling in the gaps. Trends Genet. 12, 478–483.

Rosenberg, U., Schroeder, C., Preiss, A., Kienlin, A., Kienlin, A., Coté, S., Riede, I., Jackle, H., 1986. Structural homology of the product of the *Drosophila Krüppel* gene with *Xenopus* transcription factor IIIA. Nature 319, 336–339.

Wieschaus, E.F., Nüsslein-volhard, C., Jurgens, G., 1984. Mutations affecting the pattern of the larval cuticle in *Drosophila melanogaster* III. Roux's Arch. Dev. Biol. 193, 296–307.

Wilson, M.J., Havler, M., Dearden, P.K., 2010. *Giant*, *Krüppel*, and *caudal* act as gap genes with extensive roles in patterning the honeybee embryo. Dev. Biol. 339, 200–211.